ECS Journal of Solid State Science and Technology, **7** (9) P491-P495 (2018)
2162-8769/2018/7(9)/P491/5/$37.00 © The Electrochemical Society

Thermal Atomic Layer Etching of Copper by Sequential Steps Involving Oxidation and Exposure to Hexafluoroacetylacetone

Elham Mohimi,[1] Xiaoqing I. Chu,[1] Brian B. Trinh,[2] Shaista Babar,[1] Gregory S. Girolami,[2] and John R. Abelson[1,z]

[1]*Department of Materials Science and Engineering, University of Illinois at Urbana-Champaign, Urbana, Illinois 61801, USA*
[2]*Department of Chemistry, University of Illinois at Urbana-Champaign, Urbana, Illinois 61801, USA*

We describe an atomic layer etching (ALE) method for copper that involves cyclic exposure to an oxidant and hexafluoroacetylacetone (Hhfac) at 275°C. The process does not attack dielectrics such as SiO_2 or SiN_x, and the surface reactions are kinetically self-limiting to afford a precise etch depth that is spatially uniform. Exposure of a copper surface to molecular oxygen, O_2, a weak oxidant, forms a ∼0.3 nm thick layer of Cu_2O, which is removed in a subsequent step by exposure to Hhfac. The etch reaction involves disproportionation of Cu(hfac) intermediates, such that ∼0.09 nm copper is removed per cycle. Exposure of copper to ozone, a stronger oxidant, affords ∼15 nm of CuO; when this oxidized surface is exposed to Hhfac, 8.4 nm of copper is removed per cycle. The etch products, $Cu(hfac)_2$ and H_2O, are efficiently pumped away; H_2O, a poor oxidant, does not attack the bare Cu surface. The roughness of the copper surface increases slowly over successive etch cycles. Thermochemical and bulk etching data indicate that this approach should work for a variety of other metals.
 [DOI: 10.1149/2.0211809jss]

Manuscript submitted June 27, 2018; revised manuscript received August 17, 2018. Published August 29, 2018.

Atomic layer etching (ALE) is a chemical process in which material is removed from a surface approximately one atomic layer at a time;[1–4] it is the functional opposite of atomic layer deposition (ALD). Although for many years ALE was thought to be too slow to be practical as a fabrication step for the semiconductor industry, many features in current microelectronic devices are now routinely approaching a few nm in size, and thus are in the size regime for which ALE becomes manufacturable. Furthermore, ALE is often surface selective and leads to less damage than traditional plasma etching methods. As a result, ALE is currently being investigated as a process step for the manufacture of FinFET and gate-all-around architectures. Another important potential application of ALE is in the isolation of Cu lines by removal of Cu overburden, which obviates damage to the fragile low-k interlayer dielectric during the final stages of chemical mechanical planarization.[1]

Here, we demonstrate an ALE process for copper, in which the metal surface is first oxidized and then the resulting oxide is removed in a separate step by exposure to the acidic chelating agent hexafluoroacetylacetone (Hhfac); this two-step cycle is then repeated. In each step the chemical species attacks only the target metal or its oxide overlayer, respectively, and the surface reactions are self-limiting; as a result, the process is highly surface selective and spatially uniform. The chemical steps we employ are closely related to those that have previously been used to effect the continuous etching of copper oxide, or of copper metal in which the surface is exposed simultaneously to the oxidant and an acidic chelate.[5–10] Our process differs from these previous studies in two ways: first, the exposure to the oxidant and chelating agent are sequential rather than simultaneous, thus affording much more precise control over the amount of copper that is etched. Second, our process is carried out at relatively low pressures of a few mTorr; in contrast, the previous studies were conducted at relatively high pressures of ≥10 Torr.[10]

Hexafluoroacetylacetone (Hhfac) is an attractive reagent for the ALE of metals in combination with an oxidant: the etch products, $Cu(hfac)_2$[11] and H_2O, are unreactive and simply exit the etch zone provided that the temperature is not too high. Furthermore, the system contains no reducing agent for $Cu(hfac)_2$ that would cause Cu redeposition,[12] and Hhfac does not etch SiO_2 or SiN_x.[13] An additional attribute of Hhfac is that it is unable to etch transition metals by itself because it is insufficiently oxidizing. As a result, the etch step results in the removal of the copper oxide formed by oxidation, but not the underlying copper metal.

An important requirement for ALE is that the process should be free of undesired reactions, such as ligand decomposition, which would interfere with etching or leave a deposit on the surface. It is known that, in the absence of continuous dosing, Hhfac can decompose on copper above 200°C, leaving CF_3 and ketenylidene (=C=C=O) fragments on the surface.[14] However, in studies of the use of Hhfac for the continuous etching of copper, this process either does not occur or it occurs but does not interfere with the etching.[5–9] Another study has reported that Hhfac decomposes on iron surfaces to generate surface-bound fragments containing carbon and fluorine, but these products do not interfere with etching.[15]

The copper ALE method that we describe below has the following features: (i) the etch depth is controlled to a precision as fine as 1 Å; (ii) it does not etch or damage neighboring materials such as SiO_2 or SiN_x; (iii) it uses thermal chemistry at temperatures < 300°C; (iv) the etched surface is clean and the reaction products desorb without subsequent reaction or re-deposition; and (v) the net etching rate is high enough to be practical. We demonstrate copper etch rates of 0.09 nm or 8.4 nm per cycle depending on the oxidant used.

Experimental

Experimental with O_2 as an oxidant.—The experiments were performed in a turbopumped high vacuum chamber described elsewhere.[16] Substrates consisting of E-beam evaporated Ru (10 nm)/thermal SiO_2 (300 nm)/Si were exposed to air before use, hence, the surface has converted to native RuO_x. Copper was deposited to various thickness ranging from less than 15 nm to ∼ 40 nm onto the ruthenium substrates by CVD at 100°C from the precursor Cu(hfac)(VTMS) by means of a carrier gas of 10 sccm of Ar and 1 mTorr of additional VTMS; the latter was added to reduce the roughness of the Cu surface as we previously described.[17] All gas delivery lines were pointed toward substrate; thus, the fluxes impinging on the substrate were larger than indicated by the average partial pressures. When deposited in the presence of a co-flow of VTMS, the roughness of the Cu film is 3.1 nm by AFM measurement. In addition there is a significant variation in the areal density of Cu atoms, as measured by Rutherford backscattering spectrometry (RBS): when the RBS beam is positioned in different locations, the areal density varies more than the quantity of Cu removed per cycle in the O_2 etch process (described below). It was not feasible to locate the beam in precisely the same position for successive ALE cycles. Hence, RBS could not be used to extract the etch thickness on CVD-grown Cu films; ellipsometry was used for this purpose instead (see below).

[z]E-mail: abelson@illinois.edu

Experiments using molecular O_2 were carried out without breaking vacuum. The freshly grown copper surface was exposed to molecular oxygen for 1–10 min; the chamber was evacuated for 1 min; the oxide was exposed to Hhfac for 1–6 min; and the chamber was evacuated. The partial pressure of each reactant in the chamber was fixed in the range 1–7 mTorr and the substrate temperature was fixed in the range 150–275°C. The etch product $Cu(hfac)_2$ has a high vapor pressure (10 Torr at 100°C) and was efficiently pumped away.

Oxide formation by oxygen, and etching by exposure to Hhfac, were monitored in-situ by spectroscopic ellipsometry (SE). The thicknesses of the oxide layers formed by oxidation with molecular oxygen were extracted from fits to a model based on standard multilayer optical theory, with literature values for the dielectric functions.[18] No surface or interfacial roughness is assumed in the model. Although some physical roughness does exist, detailed optical modeling has demonstrated that SE is most sensitive at a short lateral scale on the film surface, for which the roughness, evaluated by the power spectral density of AFM data, is small compared to the thickness of the oxide.[19]

Experimental with O_3 as an oxidant.—For these experiments, thicker copper films ~ 100 nm thick were deposited by E-beam evaporation onto a thermal SiO_2 (300 nm)/Si wafer, which was then cleaved into square coupons 7 mm on a side. E-beam evaporation of Cu resulted in films with as-deposited surface roughnesses of 1.3 nm as measured by AFM. In the RBS analysis, the variation in Cu areal density as a function of beam position is small compared with the etch thickness produced using O_3 as an oxidant, so that RBS could be successfully used to determine the quantity of Cu removed per etch cycle.

The coupons were placed 15 mm below a serpentine pattern low-pressure mercury lamp that generated UV photons and ozone in air.[20] Individual coupons were removed at pre-selected times up to 70 min. Separate calibrations suggest that irradiation with the mercury UV lamp causes the sample temperature to rise slowly from 28 to 40°C during the oxidation process. Oxide formation by ozone was measured by ex-situ variable angle spectroscopic ellipsometry (VASE). We found that the VASE data could not be modeled successfully using the multilayer optical theory and effective medium approximation with literature values for the dielectric functions. Trial fits were poor and not unique, probably because the surface roughness at short lateral scales is larger than the case above; this roughness may include dynamic roughening due to surface diffusion of Cu atoms. As a result, the absolute thicknesses of the oxide cannot be reliably extracted. The VASE raw data, however, are sensitive to changes in the oxide thickness, so VASE can be used reliably to detect the saturation of oxide growth, i.e., the time beyond which the data (and therefore the oxide thickness) are essentially constant.

One experiment with Hhfac was conducted using ozone-generated oxide: a coupon with a saturated oxide thickness was loaded into the high vacuum chamber and exposed to 4.5 mTorr of Hhfac at a temperature of 210°C.

Film characterization.—Film morphology was determined by cross sectional scanning electron microscopy (SEM) and atomic force microscopy (AFM). Film purity and composition were determined immediately after the oxidation or etching steps by ex situ X-ray photoelectron spectroscopy (XPS) with Mg K_α emission at 1253.6 eV. For Cu_2O, the Cu LMM Auger line is used to distinguish this phase from metallic copper (the Cu $2p_{3/2}$ binding energy is very similar).[21,22] For CuO, the Cu 2p shake-up lines are used to distinguish this oxide from Cu_2O and Cu.[22,23] Samples were briefly exposed to air during transfer from the growth chamber to the XPS chamber. To confirm that air exposure does not oxidize the etched surface, control samples of freshly grown copper were transferred using the same procedure and show no observable signals due to oxide phases.

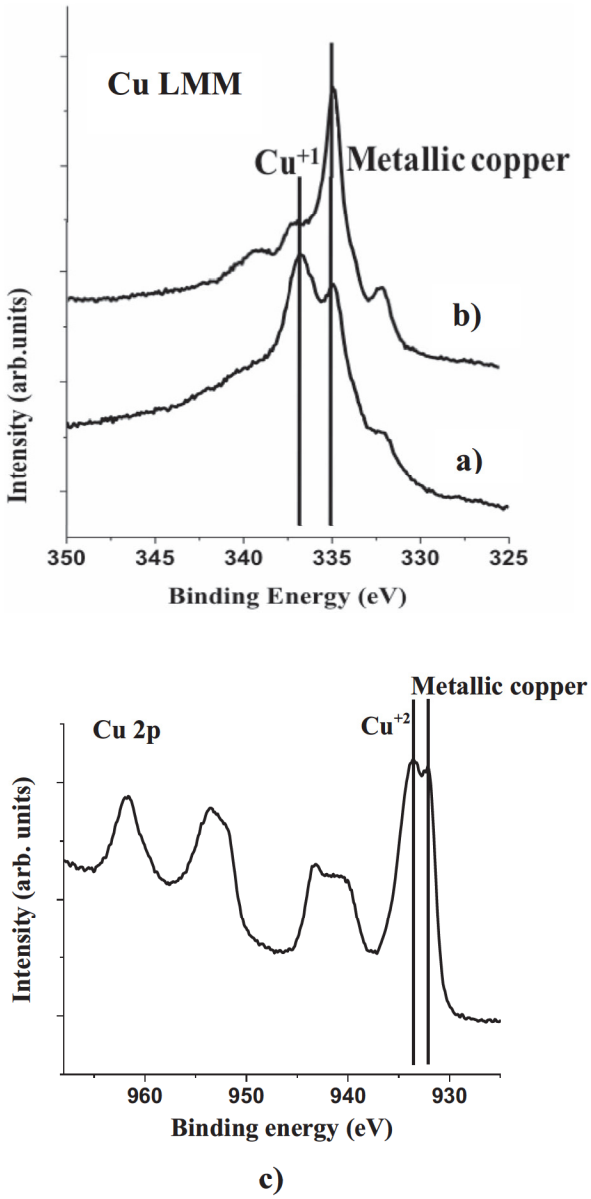

Figure 1. Cu *LMM* spectra of a) copper surface after oxidation in molecular oxygen; and b) oxygen-oxidized copper surface after etching with H(hfac). c) Cu 2*p* spectra of copper surface after oxidation in ozone. For Cu_2O, the Cu LMM Auger line is used to distinguish this phase from metallic copper because their $2p_{3/2}$ binding energies are very similar; for similar reasons, the Cu 2p shake-up lines are used to distinguish CuO, from Cu_2O and Cu.

Results

ALE of copper by sequential exposure to molecular oxygen and Hhfac.—Exposure of a copper surface to 7 mTorr of molecular oxygen for 40 min at 275°C gives a surface that, by XPS (Figure 1a), consists of copper in both 0 and +1 oxidation states (BE = 335 and 337 eV, respectively). It is well established that exposure of a copper surface to molecular oxygen under these conditions affords a layer of cuprous oxide:[24]

$$2Cu + {}^1/_2O_2 = Cu_2O \qquad [1]$$

Ellipsometry reveals that the growth rate of this cuprous oxide overlayer slows with time (Figure 2). After 8 minutes of exposure to molecular oxygen, growth of the oxide has almost stopped, and the oxide has reached a thickness of 0.3 nm; this amount corresponds to oxidation of 0.17 nm of copper metal.

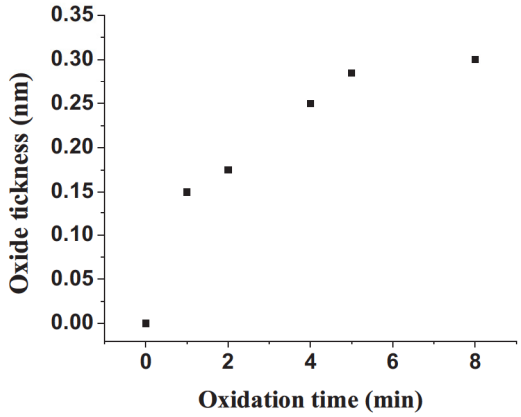

Figure 2. Oxide thickness vs. time, using 7 mTorr of O_2 at 275 °C.

Exposure of the surface oxidized in this way to 7 mTorr of Hhfac for 3 min at 275°C gives a surface that consists exclusively of copper in the metallic state (BE = 335 eV), indicating complete removal of the cuprous oxide (Figure 1b). This result is consistent with the following reaction:

$$Cu_2O + 2Hhfac = Cu(hfac)_2 + Cu + H_2O \quad [2]$$

in which the cuprous oxide disproportionates in the presence of Hhfac to one equivalent of Cu (which remains on the surface) and one equivalent of $Cu(hfac)_2$ (which desorbs and is swept away with the water co-product by vacuum pumping).[5,6] Theoretically, the removal of copper per etch cycle is equal to half of the copper contained in the Cu_2O layer.

To determine the etch rate, a 0.3 nm thick overlayer of cuprous oxide, grown by 8 min exposure of a copper surface to molecular oxygen at 275°C, was exposed at this same temperature to 7 mTorr Hhfac for varying lengths of time (Figure 3). The cuprous oxide etch rate during Hhfac exposure is nearly linear with time; the initially 0.3 nm thick oxide layer disappears after an exposure time of 2 min, giving an average oxide removal rate of 0.15 nm/min. 0.3 nm oxide, etched by Hhfac, corresponds to 0.09 nm copper. Thus, in a cyclic process that removes all the oxide during the Hhfac exposure step, the copper removal rate is 0.09 nm/cycle.

In the temperature and pressure range examined here, Hhfac does not etch metallic copper: in a control experiment, when a 37 nm thick copper film was exposed to 7 mTorr of Hhfac for 20 min at 275°C, RBS detected no change in the film thickness (above the variation due to beam position described above). This result confirms that the etching reaction is completely selective for the removal of copper oxide, consistent with previous reports.[5]

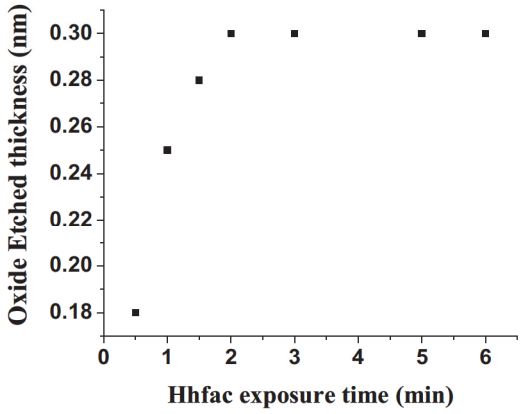

Figure 3. Etch thickness vs. H(hfac) exposure time.

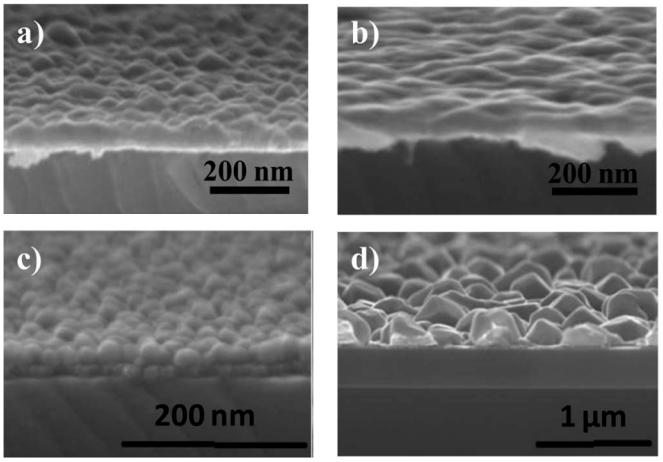

Figure 4. Cross-sectional SEM images of: a) thick copper film as grown and b) after O_2 oxidation and etch; c) thin copper film as grown and d) after O_2 oxidation and etch, where dewetting has occurred.

AFM measurements indicate that the rms surface roughness increases from 3.1 to 3.9 nm after 10 cycles of oxidation and etch. Several mechanisms may contribute to the roughness increase, and the present experiments are unable to distinguish between them. These include (i) Cu atoms released during etching of Cu_2O may be mobile and aggregate; (ii) variations in the oxidation thickness due to different crystal orientation,[25] surface defects and impurities, or due to preferential oxidation along grain boundaries;[26] or (iii) the onset of copper dewetting and agglomeration.[27]

When the copper film is thin (<15nm) (Figure 4c), a pronounced morphology change and dewetting occurs when the film is oxidized with molecular oxygen and etched with Hhfac in several cycles (Figures 4d). It is well known that a copper film will tend to dewet when a pinhole exposes the substrate surface, and that this effect is stronger in the presence of adsorbed oxygen, e.g., on SiO_2,[27] W(100),[28] and Ta[29,30] substrates. It is possible that a similar dewetting instability occurs for copper on air-exposed ruthenium. However, dewetting does not occur for thicker films that lack pinholes (Figures 4a and 4b).

ALE of copper by sequential exposure to ozone and Hhfac.—Our system is not equipped to deliver ozone in-situ, hence, we investigated the results of a single cycle of ex-situ ozone oxidation, followed by in-situ Hhfac etching. Ozone is a much stronger oxidant than molecular oxygen and affords CuO rather than Cu_2O as the room temperature

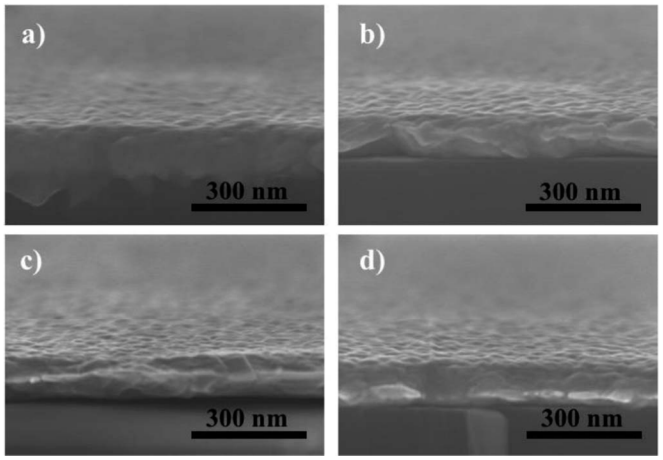

Figure 5. Cross-sectional SEM images of copper films oxidized at room temperature by ozone for different lengths of time: a) 0 min, b) 5 min, c) 20 min, and d) 40 min.

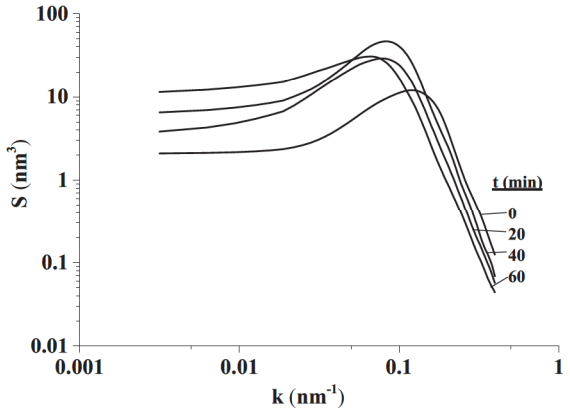

Figure 6. 2D isotropic power spectrum density S(k) as a function of oxidation time. k is the lateral separation on the surface, expressed as a wavenumber.

product; when ozone is generated in room air, the oxide surface is terminated with hydroxyl groups.[31] Figure 1c shows the Cu 2p XPS data after 70 min exposure of an E-beam evaporated copper surface to ozone at room temperature. Typical shake-up peaks at 962.0 eV and 942.2 eV, ~ 9 eV higher than the main $2p_{1/2}$ and $2p_{3/2}$ peaks, confirm that the surface contains cupric oxide, CuO. The $2p_{3/2}$ peaks at 933.6 eV and 932.4 eV indicate the presence of copper in +2 and 0 oxidation states, respectively; the latter is attributed to emission from the Cu underneath the oxide. The growth is strongly self-limiting: VASE data on different samples show that almost no change in the thickness of the CuO overlayer occurs after 20 min of oxidation by ozone under our conditions. During oxidation, the surface roughness, as inferred from SEM images (Figure 5), appears to increase slightly (Figure 6). The radially averaged power spectrum density of the AFM images (Figure 6) shows that the long-range roughness (low k) increases with oxidation time whereas the short-range roughness (high k) appears to decrease slightly, however, we did not control for the possible effect of tip blunting, i.e., we did not use a new AFM tip for each measurement).

Upon exposure of the CuO overlayer to 4.5 mTorr of Hhfac at 210°C, in-situ SE reveals that etching occurs over 2 min, after which the optical data are constant. After the etch step, no oxide is detectable by XPS; RBS data show that 8.4 nm of copper (corresponding to ~15 nm of bulk CuO) was removed in this oxidation/etch cycle. The rms surface roughness increases slightly from 1.2 nm for the cupric oxide overlayer to 1.6 nm on the bare copper that results from removal of the overlayer.

Cupric oxide is known to react with Hhfac to afford $Cu(hfac)_2$ and water:[5,6]

$$CuO + 2Hhfac = Cu(hfac)_2 + H_2O \quad [3]$$

If we assume that this same reaction is responsible for our results, the etching of cupric oxide does not involve release of Cu atoms to the film surface.

Discussion

Kinetics of copper oxidation.—A wide variety of metals exhibit self-limiting oxide growth at low temperatures: the oxide growth rate is initially very rapid, then slows as the oxide reaches a limiting thickness of ~ 10 nm.[25,32] For oxides that are electrical insulators, the classic theories of Cabrera and Mott explain this phenomenon in terms of the transport of charged defects across the oxide, which is ultimately limited by the development of an induced electric field; this mechanism leads to an inverse logarithmic growth rate which is asymptotically self-limiting.[33]

For copper, the kinetics of oxidation has been attributed to the diffusion of metal cations from the metal/oxide interface to the gas/oxide surface,[33] with only a small dependence on the pressure of molecular oxygen.[34] The oxidation of copper to Cu_2O by O_2 under our conditions shows a strongly self-limiting behavior; however, the almost discontinuous growth kinetics – a linear rise breaking over to a nearly flat saturation (Figure 2) – does not fit the inverse logarithmic law that Cabrera and Mott proposed.[33] A detailed TEM study revealed that copper oxidation by O_2 proceeds via the formation and lateral growth of Cu_2O *islands*, rather than by the growth of a uniform thickness of this oxide.[35,36] During the initial stages, copper atoms diffuse across bare areas of the surface to react at the island boundary; the limiting thickness is largely determined by the island height before coalescence. Once the islands coalesce, further transport of copper can only occur via diffusion of copper from the buried interface through the oxide, which is considerably slower. For example, oxidation of single crystal (001) Cu by 760 Torr O_2 (5 orders of magnitude greater than in the present experiments) at 70°C affords a cuprous oxide overlayer that reaches a limiting thickness of 4.5 nm.[37] The final oxide thickness is a function of the substrate temperature:[33,34] as expected, the growth rate is considerably slower below 200°C. The thickness is also a function of the crystallographic orientation of the underlying copper.[38] In the present work, the deposited copper is polycrystalline; it is not known how the distribution of surface facets on the grains may affect the limiting thickness, and therefore the uniformity, of the oxide.

For ozone as the oxidant, which converts Cu to cupric oxide, CuO, a spatially resolved study of the oxidation process is not available. Under our conditions, we find that oxidation of Cu with ozone gives 15 nm of CuO, whereas oxidation of Cu with O_2 gives only 0.3 nm of Cu_2O; this difference is consistent with the higher reactivity of ozone relative to molecular O_2. The mechanism that leads to self-limited growth of CuO from ozone is probably different from the mechanism that leads to self-limited growth of Cu_2O from O_2. In addition, it is known that the oxidation rate of copper by ozone is larger under UV exposure.[39] We generate ozone using a low-pressure mercury lamp, which inherently exposes the surface to UV photons. (Note that, if desired, ozone can be delivered to a surface, without photons, using a LN2-cooled silica-gel still with delivery through a Teflon tube;[40] this method is applicable in vacuum.)

Extension to other metals.—The present approach should be amenable to the ALE of other metals that form volatile chelate complexes: Table I lists known compounds of hfac with copper,[41] iron,[15] chromium,[42,43] nickel,[44,45] cobalt,[45] manganese,[45] zinc,[46] lead,[46,47] vanadium.[46] The enthalpies of formation, where available, indicate that the reactions of Hhfac with the corresponding metal oxides are exothermic.[45,47] Note that in some cases, the reaction stoichiometry (and thus thermodynamics) is uncertain: an example is the conversion of V_2O_5 to the vanadium(IV) product $VO(hfac)_2$.

The present approach may also be able to etch metal sulfides or nitrides: first the surface should be oxidized, releasing sulfur or nitrogen oxides, respectively; then exposure to Hhfac should remove the metal oxide, analogous to recent publications on ALE.[48] The amount of metal removed per cycle will depend on the limiting thickness of oxide; in many cases this should be well described by Mott-Cabrera kinetics.

Extension to other chelating agents.—Other chelating agents such as trifluoroacetic acid (Htfaa), and trimethylsilyl hexafluoropentanedione (SEE$^+$hfac) (which produces hexamethyldisiloxane instead of H_2O as a product) have been reported to etch iron oxide, but not elemental iron,[15] and are thus candidates for ALE.

Conclusions

We describe a general approach for thermal atomic layer etching of copper by means of sequential steps of oxidation and oxide removal by an acidic chelating agent. In agreement with previous reports, we find that the oxidation of copper is essentially self-limiting: the use of molecular oxygen at 275°C affords a ~ 0.3 nm thick Cu_2O overlayer; the use of ozone at room temperature affords a CuO layer of ~ 15 nm. In the second step, Hhfac reacts with the copper oxide to

Table I. Formation enthalpies of metal oxides and metal chelates, and calculated enthalpies for net etch reactions, at 298.15 K.

Metal	Metal oxide	Formation enthalpy (kJ/mol)	Metal chelate	Formation enthalpy (kJ/mol)	Vapor pressure at 150°C (Torr)	Net etch reaction enthalpy (kJ/mol)	References
Cu	Cu_2O	−170	$Cu(hfac)_2$	*	80	*	41
	CuO	−156					
Fe	FeO	−272	$Fe(hfac)_3$	−5115 (s)	25	−272	15
	Fe_2O_3	−826				(Fe_2O_3)	
	Fe_3O_4	−1121					
Ni	NiO	−240	$Ni(hfac)_2 \cdot 2H_2O$	−4003†	*	−235	44,45
Cr	Cr_2O_3	−1135	$Cr(hfac)_3$	−5359‡	30	−451	42,43
Pb	PbO	−219	$Pb(hfac)_2$	−3192	*	−29	46,47
Zn	ZnO	−351	$Zn(hfac)_2$	*	*	*	46
V	V_2O_5	−1551	$VO(hfac)_2$	*	*	*	46
Mn	MnO	−385	$Mn(hfac)_2 \cdot 2H_2O$	−4163†	*	−250	45
Co	CoO	−238	$Co(hfac)_2 \cdot 2H_2O$	−4009†	9	−243	45
Hhfac				−1643			45
H_2O				−242			45

*not reported.
†±10 kJ/mol.
‡±17 kJ/mol.

form $Cu(hfac)_2$; this step is fully self-limiting because Hhfac reacts with the copper oxide layer of limited thickness rather than the copper underneath. The overall process is perfectly selective for the etching of metals, so that SiO_2 or SiN_x on the substrate surface are not removed. We suggest, based on thermochemical data and the 'cleaning' literature, that a variety of other metals can be etched by this method, and that non-halogenated chelating agents could be substituted for Hhfac.

Acknowledgments

G.S.G. thanks the National Science Foundation for support of this research under grant CHE 1665191. J.R.A. acknowledges support from the National Science Foundation under grants DMR 1005715 and DMR 1410209. Compositional and structural analyses of the films were carried out in part in the Frederick Seitz Materials Research Laboratory Central Research Facilities, University of Illinois.

ORCID

Xiaoqing I. Chu https://orcid.org/0000-0003-3184-3847
John R. Abelson https://orcid.org/0000-0002-9040-1910

References

1. C. T. Carver, J. J. Plombon, P. E. Romero, S. Suri, T. A. Tronic, and R. B. Turkot, *ECS J. Solid State Sci. Technol.*, **4**, N5005 (2015).
2. S. T. K. J. Kanarik, J. Holland, A. Eppler, V. Vahedi, J. Marks, and R. A. Gottscho, *Solid State Technol.*, **56**, 14 (2013).
3. K. J. Kanarik, T. Lill, E. A. Hudson, S. Sriraman, S. Tan, J. Marks, V. Vahedi, and R. A. Gottscho, *J. Vac. Sci. Technol., A*, **33**, 020802 (2015).
4. G. S. Oehrlein, D. Metzler, and C. Li, *ECS J. Solid State Sci. Technol.*, **4**, N5041 (2015).
5. M. A. George, D. W. Hess, S. E. Beck, J. C. Ivankovits, D. A. Bohling, and A. P. Lane, *J. Electrochem. Soc.*, **142**, 961 (1995).
6. A. Jain, T. T. Kodas, and M. J. HampdenSmith, *Thin Solid Films*, **269**, 51 (1995).
7. A. Sekiguchi, A. Kobayashi, T. Koide, O. Okada, and N. Hosokawa, *Jpn. J. Appl. Phys.*, **39**, 6478 (2000).
8. S.-W. Kang, H.-U. Kim, and S.-W. Rhee, *J. Vac. Sci. Technol., B*, **17**, 154 (1999).
9. W. Lee, H.-J. Yang, P. J. Reucroft, H.-S. Soh, J.-H. Kim, S.-L. Woo, and J. Lee, *Thin Solid Films*, **392**, 122 (2001).
10. R. Steger and R. Masel, *Thin Solid Films*, **342**, 221 (1999).
11. B. D. Fahlman and A. R. Barron, *Adv. Mater. Opt. Electron.*, **10**, 223 (2000).
12. S. L. Cohen, M. Liehr, and S. Kasi, *Appl. Phys. Lett.*, **60**, 50 (1992).
13. R. F. Riley, R. West, R. Barbarin, G. Slusarczuk, and S. Kirschner, *Inorg. Synth.*, **7**, 30 (1963).
14. G. S. Girolami, P. M. Jeffries, and L. H. Dubois, *J. Am. Chem. Soc.*, **115**, 1015 (1993).
15. M. A. George, D. W. IIess, S. E. Beck, K. Young, D. A. Bohling, G. Voloshin, and A. P. Lane, *Journal of The Electrochemical Society*, **143**, 3257 (1996).
16. S. Jayaraman, Y. Yang, D. Y. Kim, G. S. Girolami, and J. R. Abelson, *J. Vac. Sci. Technol., A*, **23**, 1619 (2005).
17. S. Babar, L. M. Davis, P. Zhang, E. Mohimi, G. S. Girolami, and J. R. Abelson, *ECS J. Solid State Sci. Technol.*, **3**, Q79 (2014).
18. E. D. Palik, in *Handbook of Optical Constants of Solids*, p. 3, Academic Press, Burlington (2002).
19. B. A. Sperling and J. R. Abelson, *Appl. Phys. Lett.*, **85**, 3456 (2004).
20. E. R. Santos, E. C. Burini, and S. H. Wang, *Ozone-Sci. Eng.*, **34**, 129 (2012).
21. E. Apen, B. R. Rogers, and J. A. Sellers, *J. Vac. Sci. Technol., A*, **16**, 1227 (1998).
22. C. D. Wagner and G. E. Muilenberg, *Handbook of X-ray photoelectron spectroscopy: a reference book of standard data for use in X-ray photoelectron spectroscopy*, Physical Electronics Division, Perkin-Elmer Corp., Eden Prairie, Minn. (1979).
23. P. D. Kirsch and J. G. Ekerdt, *J. Appl. Phys.*, **90**, 4256 (2001).
24. Y. S. Gong, C. P. Lee, and C. K. Yang, *J. Appl. Phys.*, **77**, 5422 (1995).
25. T. N. Rhodin, *J. Am. Chem. Soc.*, **73**, 3143 (1951).
26. G. Zhou and J. C. Yang, *J. Mater. Res.*, **20**, 1684 (2011).
27. H. Y. Liao, K. J. Lo, and C. C. Chang, *Nanotechnology*, **20**, 465607 (2009).
28. A. J. Melmed, *J. Appl. Phys.*, **37**, 275 (1966).
29. L. Chen, N. Magtoto, B. Ekstrom, and J. Kelber, *Thin Solid Films*, **376**, 115 (2000).
30. J. W. Bae, J.-W. Lim, K. Mimura, and M. Isshiki, *Mater. Trans.*, **45**, 877 (2004).
31. S. Bok, G. H. Lim, and B. Lim, *J. Ind. Eng. Chem.*, **46**, 199 (2017).
32. T. N. Rhodin, *J. Am. Chem. Soc.*, **72**, 5102 (1950).
33. N. Cabrera and N. F. Mott, *Rep. Prog. Phys.*, **12**, 163 (1948).
34. A. U. Seybolt, *Adv. Phys.*, **12**, 1 (1963).
35. J. C. Yang, B. Kolasa, J. M. Gibson, and M. Yeadon, *Appl. Phys. Lett.*, **73**, 2841 (1998).
36. G. Zhou, L. Luo, L. Li, J. Ciston, E. A. Stach, W. A. Saidi, and J. C. Yang, *Chem. Commun. (Camb.)*, **49**, 10862 (2013).
37. F. W. Young, J. V. Cathcart, and A. T. Gwathmey, *Acta Metall.*, **4**, 145 (1956).
38. J. Gao, A. Hu, M. Li, and D. Mao, *Appl. Surf. Sci.*, **255**, 5943 (2009).
39. H. Lin and G. S. Frankel, *Corros. Eng. Sci. Technol.*, **48**, 461 (2013).
40. S. Oh and J. N. Eckstein, *Thin Solid Films*, **483**, 301 (2005).
41. M. W. Chase, and National Institute of Standards and Technology (U.S.), *NIST-JANAF thermochemical tables*, American Chemical Society, Washington, D.C.; American Institute of Physics for the National Institute of Standards and Technology, Woodbury, N.Y. (1998).
42. Y. Harada and G. S. Girolami, *Polyhedron*, **26**, 1758 (2007).
43. M. A. V. R. Da Silva and M. L. C. C. H. Ferrão, *J. Chem. Thermodyn.*, **19**, 645 (1987).
44. H. L. Nigg and R. I. Masel, *J. Vac. Sci. Technol., A*, **17**, 3477 (1999).
45. M. A. V. R. Da Silva and M. L. C. C. H. Ferrão, *Thermochim. Acta*, **139**, 33 (1989).
46. F. Rousseau, A. Jain, T. T. Kodas, M. Hampden-Smith, J. D. Farr, and R. Muenchausen, *J. Mater. Chem.*, **2**, 893 (1992).
47. V. V. Krisyuk, S. V. Sysoev, N. E. Fedotova, I. K. Igumenov, and N. V. Grigorieva, *Thermochim. Acta*, **307**, 107 (1997).
48. Y. Lee and S. M. George, *Chem. Mater.*, **29**, 8202 (2017).